Economic-Environmental Analysis of Combined Heat and Power-Based Reconfigurable Microgrid Integrated with Multiple Energy Storage and Demand Response Program

Mohammad Hemmati[1], Mohammad Amin Mirzaei[1], Mehdi Abapour[1], Kazem Zare[1], Behnam Mohammadi-ivatloo[1,2], Hassan Mehrjerdi[3], Mousa Marzband[4]

[1]Faculty of Electrical and Computer Engineering, University of Tabriz, Tabriz, Iran
[2] Department of Energy Technology, Aalborg University, 9220 Aalborg, Denmark
[3] Electrical Engineering Department, Qatar University, Doha, Qatar
[4] Department of Mathematics, Physics and Electrical Engineering, Northumbria University, Newcastle, England

Abstract

Microgrids (MGs) are solutions to integrate high shares of variable renewable energy which can contribute to more economical and environmental benefits, as well as improving the energy supply efficiency. One significant potential of MGs is an expanded opportunity to use the waste heating energy from the conversion of the primary fuel (such as natural gas) to generate electricity. The use of waste heat in combined heat and power (CHP)-based MG is more efficient to meet local load and decrease the emission pollution. Hence, this paper elaborates on optimal multi-objective scheduling of CHP-based MG coupled with compressed air energy storage (CAES), renewable energy, thermal energy storage (TES), and demand response programs through shiftable loads, which considers a reconfiguration capability. The embedded CAES, in addition to the charging/discharging scheme, can operate in a simple cycling mode and serve as a generation resource to supply local load in an emergency condition. The daily reconfiguration of MG will introduce a new generation of MG named reconfigurable microgrid (RMG) that offers more flexibility and enhances system reliability. The RMG is coupled with TES to facilitate the integration of the CHP unit that enables the operator to participate in the thermal market, in addition to the power market. The main intents of the proposed multi-objective problem are to minimize the operation cost along with a reduction in carbon emission. The epsilon-constraint technique is used to solve the multi-objective problem while fuzzy decision making is implemented to select an optimal solution among all the Pareto solutions. The electricity prices and wind power generation variation are captured as random variables in the model and the scenario-based stochastic approach is used to handle them. Simulation results prove that the simultaneous integration of multiple technologies in CHP-based RMG decreases the operation cost and emission up to 3% and 10.28%, respectively.

Keywords- Reconfigurable microgrid, multi-objective optimization, compressed air energy storage, emission.

Nomenclature

Index:

t	Index for time
i	Index for MTs
l	Index for electrical demand
w	Index of wind turbines
s	Index for scenarios
b, b'	Index buses
L	Index of feeders
K	Index for switches
lp	Index for loops
u	Index of minimum on/ off time limits from 1 to $\max\{MUT_i, MDT_i\}$

Constants:

$\theta_{b,b'}$	The value of impedance angle (degree)
$Z_{b,b'}$	The line Impedance between b and b' (Ω)
eh^{CH} / eh^{D}	Charging/ discharging efficiency of thermal storage
$g^{i} / g^{chp} / g^{m} / g^{dis} / g^{sc}$	Emission factor of micro-turbine/ CHP/ power purchased/ CAES in discharging mode/ CAES in simple cycle mode
ER	Energy ratio of CAES
a_1, a_2, a_3	Generation coefficient of wind turbine
HR^{dis} / HR^{sc}	Heat rate during discharging/ simple cycle mode
LPF	Load participation factor
$S_{\max}^{\exp}$	Maximum power of the expander (kVA)
$P^{ch,\max} / P^{dis,\max} / P^{sc\max}$	Maximum power charging/ discharging/ simple cycle of CAES (kW)
$P_i^{\max}, P_i^{\min}$	Min/Max active power of MT (kW)

$Q_i^{\max}, Q_i^{\min}$	Min/Max reactive power of MT (kVAr)
$V^{\min} / V^{\max}$	Min/max value of bus voltage (p.u.)
UT^{chp} / DT^{chp}	Min up/downtime for CHP (hour)
$E^{\min} / E^{\max}$	Min/max capacity of CAES (kWh)
$HS^{\min} / HS^{\max}$	Min/max energy capacity of TES (kWh)
$P^{chp,min} / P^{chp,max}$	Min/max power output of the CHP (kW)
$H^{D,\min} / H^{D,\max}$	Min/max produced heat by TES (kW)
$H^{CH,\min} / H^{CH,\max}$	Min/max heating charged in TES (kW)
π_{NG}	Natural gas price (¢/Mbtu)
NB	Number of buses
NL	Number of loads
NLI_{lp}	Number of lines in a possible loop
NCS_{lp}	The initial number of closed switches before reconfiguration
NPL_{lp}	Required number of lines to make a loop
NU	Number of MT units
NS	Number of scenarios
NT	Number of time intervals
$VOM^{\exp} / VOM^{c}$	Operation and maintenance cost of expander/compressor (¢/kWh)
$R^{chp,Up} / R^{chp,Dn}$	Ramp-up/ramp down of CHP (kW/h)
R_i^{dn} / R_i^{up}	Ramp up/down of MT unit *i* (kW/h)
MUT_i / MDT_i	Min up/downtime of MT
P_w^R	Rated active power of wind plant (kW)
S_L	The capacity of line *L* (kVA)
S_w	The total power produced by a wind turbine (kVA)
SDC_i / SUC_i	Shut down/ Start-up cost of MT *i* (¢/kWh)
C^{dr}	Cost of DR (¢/kWh)
C^{curt}	Cost of wind power curtailment (¢/kWh)
eh	Heat loss coefficient of thermal storage

M	Massive auxiliary number
$DR_{l,m,s}^{\max}$	Maximum shiftable demand (kW)
$H^{chp,A}$ / $H^{chp,B}$ / $H^{chp,c}$ / $H^{chp,D}$	Heat output of the CHP based on operation region (kW)
$P^{chp,A}$ / $P^{chp,B}$ / $P^{chp,C}$ / $P^{chp,D}$	The power output of the CHP based on operation region (kW)

Variables:

$PF_{L,t,s}$	Line active power flow (kW)
$QF_{L,t,s}$	Line reactive power flow (kVAr)
$D_{l,t,s}^{DR}$	Active responsible load value participates in DRP (kW)
$Q_{l,t,s}^{DR}$	Reactive responsible load value participates in DRP (kVAr)
I_t^{chp} / I_{t-1}^{chp}	A binary variable for on/off status of CHP
$I_{i,t}$	A binary variable for on/off status of MT
$K_{L,t,s}$	Binary variable equals 1 if the switch is closed, otherwise is 0
$u_{t,s}^{ch}$ / $u_{t,s}^{dis}$ / $u_{t,s}^{sc}$	Binary variable for charging/ discharging/ simple cycle mode of CAES
$V_{b,t,s}$	Voltage magnitude
$C(P_{i,t,s})$	The cost function of MT unit i
$Ih_{t,s}^{D}$ / $Ih_{t,s}^{CH}$	Discharging/charging binary variable for heat storage (kW)
$E_{t,s}$	The energy capacity of CAES (kWh)
$P_{i,t,s}$	Active power output by MT (kW)
$Q_{i,t,s}$	Reactive power output by MT (kVAr)
$\lambda_{t,s}^{em}$	Market price (¢/kWh)
$T^{chp,on}$ / $T^{chp,off}$	Number of successive on/off hours of CHP (hour)
OF_1 / OF_2	Objective functions
$P_{w,t,s}^{curt}$	Power curtailment of wind turbine w (kW)
$P_{t,s}^{buy}$ / $P_{t,s}^{sell}$	Purchased/sold active power from/ to the grid (kW)
Q_t^{upstr}	Reactive power exchanged with the upstream network (kVAr)

$Q^{\exp}_{t,s}$	Reactive power of expander (kVAr)
π_s	Scenario probability
$H^{buy}_{t,s}$ / $H^{sell}_{t,s}$	Purchased/sold thermal from/to the thermal market (kW)
$SU_{i,t}, SD_{i,t}$	Start-up/shut-down costs related to MT (¢/kWh)
$H^{D}_{t,s}$ / $H^{CH}_{t,s}$	Discharged/charged heating by TES (kW)
$H^{chp}_{t,s}$	Generated heat by CHP (kW)
$P^{chp}_{t,s}$ / $P^{chp}_{t-1,s}$	Generated power by CHP (kW)
$HS_{t,s}$ / $HS_{t-1,s}$	Heat capacity of TES (kWh)
$P^{ch}_{t,s}$ / $P^{dis}_{t,s}$ / $P^{sc}_{t,s}$	Charged/dischared/generated power by by CAES during charging/discharging/simple-cycle mode (kW)
λ^{hm}_{t}	Thermal market price (¢/kWh)
$\delta_{b,t,s}$	Voltage angle of the bus (degree)
$P^{f}_{w,t,s}$	Wind active power output (kW)
$Q^{f}_{w,t,s}$	Wind reactive power output (kVAr)

1. Introduction

1.1. Motivation

Microgrid (MG), which was primarily introduced to mitigate the integration of distributed generations (DGs) in the distribution system, offers multiple goals for utility, and consumers, including a reduction in greenhouse emission, power loss, and operation cost, and improving system flexibility and reliability [1]. Combined heat and power (CHP) systems are becoming very popular in the MGs. The CHP unit generates both thermal and electrical energy, simultaneously, which enhances the optimal operation of the system. The CHP-based MG provides much higher flexibility by supporting both electrical and heating loads and offers a suitable opportunity for the system operator to participate in the thermal market, in addition to the electricity market. Furthermore, providing a flexible structure through reconfigurable capability for CHP-based MG will give additional benefits to consumers, MG's owner, and utility. The optimal structure of MG could be achieved by changing the status of embedded tie-switches in MG's structure via a reconfiguration capability. The reconfigurable microgrid (RMG) is a new generation of conventional MG that optimizes the hourly structure of MG to diminish the power loss, as well as operation cost [2]. Compressed air energy storage system (CAES) with unique features like higher efficiency, no dependency on geographical conditions, and one more operation mode can be integrated into the CHP-based RMG model to support the more renewable energy utilization, as well as carbon dioxide reduction [3]. Integrated CHP-based MG with CAES facility by considering charging, discharging, and simple cycle operation modes can satisfy economic and environmental benefits. Also, the demand response program (DRP) is introduced as a new capability to improve load managing and flexibility, which has been much attention in the modern power system like RMGs. The incentive-based DRP provides the opportunity for consumers to participate in the management of MG and receive encouragement in their bills via shifting their energy consumption from peak hours to off-peak intervals. Given that MG often utilizes renewable energy and participates in the electricity market to meet the required energy, along with hourly load variation, the optimal operation of MG is exposed to high-level uncertainty caused by electricity price, load, and renewable energy output. Therefore, the implementation of a more accurate and realistic optimization approach to capture all random variables in the model is urgently needed.

Toward the goals of CHP-based MG scheduling in economical and reliable ways have been investigated recently, there are still several shortcomings in this field that need to be developed. An essential issue of the CHP-based MG operation is to consider the reconfigurable capability, integrated DRP, as well as CAES and TES facilities in this system to supply both electrical and heating loads, and participate in both electrical and thermal markets with an appropriate optimization framework.

1.2. Literature review

The MG optimal operation is extensively studied in the literature. The MG energy management in grid-connected mode by considering the unit commitment and reconfiguration to maximize the profit was developed by [4]. A grid-connected MG scheduling based on economic and environmental goals was investigated by [5]. Optimal energy management of islanding MG with the aim of the emission cost, battery degradation cost, and generation minimization was studied in [6]. The proposed approach was formulated as a chance-constrained optimization model, and an ambiguity set approach was applied to manage the uncertainty of renewable power output. The coordinated energy dispatch model of a multi-carrier MG in both islanded and grid-connected modes in the presence of the CHP, fuel cell, gas boiler, and renewable generation units was presented by [7] to minimize total operational cost. In [8], the optimal energy planning of autonomous hybrid MG to minimize operation and investment costs were evaluated based on the multi-objective optimization approach. An integrated multi-objective optimization framework to minimize the operational cost and gas emission in MG was investigated in [9]. The optimal scheduling of RMG integrated with wind and solar energy based on the chance-constrained model was developed by [10]. The authors of [11] investigated the coordination of photovoltaic (PV) resources and combined cooling, heat, and power (CCHP) unit in the grid-connected MG to minimize the operating cost. In [12], a residential CCHP-based MG consisting of hybrid electric vehicles, PV, and battery energy storage systems was investigated to determine the optimal sets' points of multiple generation units by considering the market price, electrical and thermal demand, and PV power output fluctuation, based on a scenario-based stochastic approach. Authors in [13] studied the CCHP-based MGs energy dispatch model. The proposed scheduling was reformulated as a two-stage optimization approach to achieve a more economic benefit. The economic dispatch model of CHP-based MG under the network-constrained problem was studied in [14]. The proposed network-constrained model was reformulated as a mixed-integer non-linear programming (MINLP) model.

Recently, DRP applications as flexible, emerging resources to satisfy technical and economic benefits have been extensively developed in the literature. In [15], a smart renewable-based MG optimal operation with responsible loads was evaluated. The shiftable demands participate in DRP via the time-of-use (TOU) and real-time pricing (RTP) models as two main DRPs. A dynamic price-based DRP integrated into grid-connected MG operation incorporated with wind energy was investigated by [16]. The economic dispatch model for the islanded MG integrated with DRP, considering the forecasting error of renewable energy, was analyzed by [17]. Authors in [18] implemented the DRP to mitigate the challenges resulting from the mismatch issues between generation and consumption in an islanded renewable-based MG. The MG optimal operation integrated with incentive-based DRP to minimize the operation cost, considering renewable energy output, load consumption, and line outages uncertainties have been studied in [19].

Bulk energy storage technologies can provide more benefits for both utility and end-users, such as peak-shaving, load shifting, more renewable energy integration, and ancillary services. The CAES facility is one of the high-efficient and large-scale energy storage technology that is especially important in an age where variable renewable energy like wind power is becoming a more prominent energy resource. The basic CAES facility operation is the thermodynamic cycle, which compresses the air during charging mode, and releases the high-pressure air at discharging mode to generate power during peak interval to meet higher demand. In addition to the charge and discharge scheme, the CAES facility can operate as a micro-turbine when the air cavern is depleted, named simple cycle operation mode [20]. This unique feature makes the CAES facility different from other technologies. Integration of CAES in MG while provides more economical and environmental benefits; it can operate as a local power plant in simple cycle mode to meet higher demand. Due to the fast response, small environmental effects, and great economic benefits, the CAES facility is a suitable solution for an isolated area like MG [21]. The optimal bidding and offering strategies of CAES with a smart charging-discharging scheme based on a robust-stochastic approach was developed by [22]. An islanded MG planning integrated with renewable Energy and CAES facility was investigated by [23]. The integration of CAES and DRP in day-ahead MG operation incorporated with flexible ramping products was developed by [24]. In this work, the IGDT-based robust framework was investigated to manage the wind power variation.

The energy supply and electricity generation are key contributors to greenhouse emissions and climate change. Hence, the optimal operation of MG from an environmental perspective should be captured. In [25], the economic/ emission dispatch model of islanded and renewable-based MG based on a multi-objective framework was studied. The stochastic multi-objective economic/ environmental optimal scheduling of MG incorporated with the battery was studied in [26]. In this work, a meta-heuristic algorithm based on differential evolutionary and modified PSO was implemented to solve the problem. In [27], a multi-objective optimization model of CHP-based MG in the presence of renewable energy, fuel-cell, and heat storage was investigated. The proposed MG can exchange the power and heat with the main grid and district heating network. The multi-objective operation of CHP-based MGs incorporated with electrical energy storage and DRPs with the aim of total operational cost and emission pollution minimization was developed by [28]. The proposed model was reformulated as a mixed-integer linear model, while the Ɛ-constraint method was used to find an optimum solution. The multi-objective economic and environmental scheduling of CHP-based MG integrated with the fuel-cell unit, thermal storage, and DRP was studied in [29]. In the presence of load and power price variability, the epsilon-constraint method was applied to find an optimum solution to the multi-objective scenario-based stochastic problem. In [30], a renewable and CHP-based MG power dispatch scheduling was developed to minimize generation cost, emission, and reliability cost based on the energy not-supplied index. To solve the proposed multi-objective program contains three different objectives, the weighted sum method, and an exchange market algorithm was implemented.

Meanwhile, the penetration of renewable power generation, and load variation, is one of the most common challenges faced by MGs operation [31]. In [32], a probabilistic optimization approach was investigated for optimal operation of CHP-based MGs integrated with DRP, with the load, energy price, and wind power output uncertainty. The optimal operation of CHP-based MG with high-level uncertainty from load demand, wind energy, and market price, was evaluated by [33]. A new stochastic p-robust optimization framework was extended to handle system uncertainties. The risk-based optimal scheduling of the RMG with the high penetration of wind energy to maximize daily profit, with the wind power and market price variability, was developed by [34]. The optimal MGs design, considering the flexible structure using the reconfiguration process based on a robust optimization approach, was evaluated in [35]. In [36], a novel two-stage optimization approach for the flexible operation of RMG in real-time and day-ahead markets was developed, considering wind energy, load, and market price variation.

1.3. Novelty and contribution

The literature review indicated the importance of CHP-based MG operation integrated with renewable energy. However, there has been no discussion about a comprehensive model for optimal operation of CHP-based MG while considers the reconfiguration ability, multiple energy storage, and DRP to enhance the flexibility and efficiency of energy supply. Motivated by economic and environmental challenges, this paper proposes a novel two-stage multi-objective stochastic scheduling of CHP-based RMG integrated with CAES, wind energy, TES, micro-turbines (MTs), and incentive-based DRP to meet local electrical demands. The power price and generated power by wind turbines are associated with uncertainty, and the stochastic approach is implemented to manage them. In addition to the charge and discharge scheme, the simple cycle mode is considered for the CAES operation when the cavern air is depleted, which provides more flexibility for the system. The proposed RMG relying on local resources participates in both electrical and thermal markets and has energy exchanged (selling and purchasing) with the corresponding market. Also, the AC-power flow equation is extended to realize the limitation of RMG topology in detail. The main contribution of this work can be summarized as follows:

1. Eco-emission analysis of optimal hourly switching in the reconfigurable CHP-based MG considering the C-power flow, and security constraints. Reconfiguration capability by adjusting the hourly switches' status, transfers the demand from heavily loaded pats to lightly ones contributing to more economic and environmental benefits.

2. Analyzing the environmental and economic operation of reconfigurable CHP-based MG as a multi-objective optimization problem to reveal the role of effective integration of flexible technologies in the MG model from economic and emission pollution perspectives.

3. Coordinated operation of the DRP, tri-state CAES, TES, reconfigurable capability, and wind plant as flexible resources in the proposed scheduling to provide more economical and environmental benefits. In this way, while the individual scheduling of each resource has been studied, the simultaneous integration of all of the technologies in this study results in daily cost reduction, as well as a large amount of carbon dioxide reduction.

4. Evolving the strong uncertainty of wind power and power price to more realistic modeling of the reconfigurable CHP-based MG under the two-stage stochastic approach. Furthermore, the effects of simultaneous integration of several technologies in the proposed model are investigated, unlike the previous studies that focused on the individual coordination of these facilities.

To demonstrate the novelty of our work, Table I compares the main contributions with similar works.

Table I. Comparison of novelty and contributions of the proposed model with similar works.

Ref	CHP-based MG scheduling	Network constraint modeling	Reconfigurable capability	Objective		Main components			DRP	Uncertainty modeling
				economic	Emission	TES	CAES	RES		
[7]	✓	—	—	✓	—	✓	—	✓	—	Deterministic
[11]	✓	—	—	✓	—	—	—	✓	—	Stochastic
[14]	✓	AC-OPF	—	✓	—	—	—	✓	—	Robust/ stochastic
[23]	—	—	—	✓	—	—	✓	✓	—	Deterministic
[25]	—	—	—	✓	✓	—	—	✓	—	Stochastic
[26]	—	—	—	✓	✓	—	—	✓	✓	Stochastic
[27]	✓	—	—	✓	✓	✓	—	✓	—	Deterministic
[28]	✓	—	—	✓	✓	—	—	✓	✓	Deterministic
[29]	✓	—	—	✓	✓	✓	—	✓	✓	Stochastic
[30]	✓	—	—	✓	✓	—	—	✓	—	Stochastic
[32]	✓	—	—	✓	—	—	—	✓	✓	Stochastic
[34]	—	AC-OPF	✓	✓	—	—	—	✓	—	Stochastic
[35]	—	AC-OPF	✓	✓	—	—	—	✓	—	Robust
[37]	—	AC-OPF	✓	✓	—	—	—	—	✓	Deterministic
[38]	—	AC-OPF	✓	✓	—	—	—	—	—	Deterministic
[39]	✓	Based MATPOWER	Only for connection between neighboring MG	✓	—	—	—	✓	✓	Stochastic
Our work	✓	AC-OPF	✓	✓	✓	✓	✓	✓	✓	Two-stage Stochastic

1.4. Paper organization

The rest of this paper is organized as follows. The problem description and formulation, including both economic and emission objective functions with corresponding restrictions, are presented in Section 2. The solution method to solve the proposed two-stage multi-objective problem is represented in Section 3. Numerical results are discussed in Section 4, and Section 5 concludes the paper.

2. Problem description and formulation

The optimal operation of CHP based MG considering reconfiguration to minimize operational cost and emission pollution to satisfy electrical loads incorporated with incentive-based DRP, TES, and CAES facility is formulated as a multi-objective two-stage stochastic optimization problem subject to technical and operational constraints. The RMG's operator participates in the power market to supply local loads while the heat generation equipment such as CHP unit and TES allows the operator to participate in the thermal market, too. Fig. 1 describes the overall schematic of the proposed scheduling of renewable and CHP-based RMG integrated with multiple components. As can be seen, the RMG's operator optimizes the operation of local generation units, including CAES, CHP, TES, MTs, and makes a contract with responsible loads. Meanwhile, the operator tends to participate in energy markets. Hence, by analyzing the power and thermal market conditions, the operator decides on power and heating exchanged (selling or purchasing) with electricity and thermal markets. It should be noted that the operator must manage the variability of electricity price and wind energy by a scenario-based stochastic approach. By optimizing the operation of local resources, hourly topology, hourly energy exchanged, and hourly scheduling of responsible loads, the operator can satisfy the economic and environmental benefits.

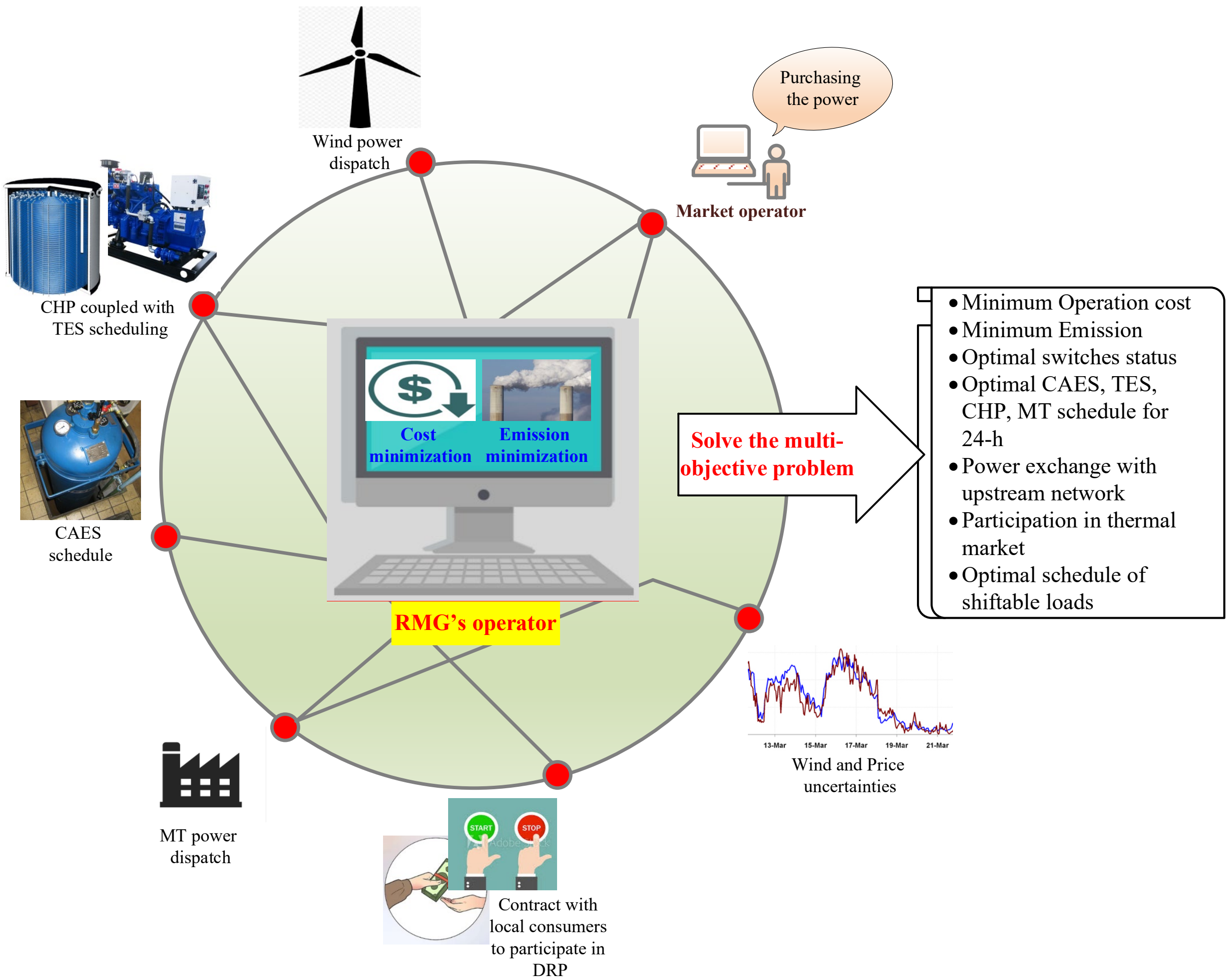

Fig. 1. The proposed multi-objective optimization problem of renewable and CHP-based RMG.

Two objective functions for economic cost and emission goals are represented in the following.

2.1. Objective function

The first objective function related to operational cost minimization is represented by (1). The first term in the objective function (1) refers to the start-up and shut-down costs of MTs. The start-up and shut-down costs of the CHP are expressed in the next term (1). The power exchanged (selling or purchasing) with the upstream network is shown by the third term of the objective function (1). The heating exchanged (selling or purchasing) with the thermal market is represented by the next term (1). The fifth and sixth terms of (1) signify the generation costs of MT and CHP units, respectively. In this paper, the generation cost of MT is represented by the quadratic function as [40]. Also, the generation cost of the CHP unit is represented by a linear function [41]. The seventh, eighth, and ninth terms of the objective function (1) are related to the operation cost of the CAES facility in discharging, simple cycle, and charging modes, respectively. Finally, the last line of the objective function (1) deals with load shedding DRP cost, as well as wind curtailment cost.

$$OF_1 = \min \left(\begin{array}{l} \sum_{t=1}^{NT}\sum_{i=1}^{NU}\left(SU_{i,t}+SD_{i,t}\right)+\sum_{t=1}^{NT}\left(SU_t^{chp}+SD_t^{chp}\right) \\ +\sum_{s=1}^{NS}\pi_s \left(\begin{array}{l} \sum_{t=1}^{NT}\lambda_{t,s}^{em}\left(P_{t,s}^{buy}-P_{t,s}^{sell}\right)+\sum_{t=1}^{NT}\lambda_t^{hm}\left(H_{t,s}^{buy}-H_{t,s}^{sell}\right)+\sum_{t=1}^{NT}\sum_{i=1}^{NU}C\left(P_{i,t,s}\right) \\ +\sum_{t=1}^{NT}C\left(P_{t,s}^{chp},H_{t,s}^{chp}\right)+\sum_{t=1}^{NT}\left(\left[P_{t,s}^{dis}\times\left(HR^{dis}\times\pi^{NG}+VOM^{\exp}\right)\right]\right. \\ \left.+\left[P_{t,s}^{sc}\times\left(HR^{sc}\times\pi^{NG}+VOM^{\exp}\right)\right]+\left[P_{t,s}^{ch}\times VOM^{c}\right]\right) \\ +\sum_{t=1}^{NT}\sum_{l=1}^{NL}C^{dr}\left|DR_{l,t,s}\right|+\sum_{t=1}^{NT}\sum_{w=1}^{NW}C^{curt}P_{w,t,s}^{curt} \end{array} \right) \end{array} \right) \tag{1}$$

The handling of carbon emission pollution based on the environmental standards should be considered for the fossil-based unit (usually natural gas-fired units), including CHP, MTs, and CAES (during discharging and simple cycle operation modes). Hence, the objective function related to emission pollution minimization is formulated as (2).

$$OF_2 = \min \sum_{s=1}^{NS}\pi_s\left(\sum_{t=1}^{NT}\left[\sum_{i=1}^{NU}\left(\gamma^i P_{i,t,s}\right)+\gamma^{chp}P_{t,s}^{chp}+\gamma^{Dis}P_{t,s}^{Dis}+\gamma^{sc}P_{s,t}^{sc}+\gamma^{em}P_{t,s}^{buy}+\gamma^{hm}H_{t,s}^{buy}\right]\right) \tag{2}$$

The objective function in (2) contains seven terms. The emission pollution by MTs and CHP units are represented in the first and second terms of (2), respectively. The CAES facility uses the fuel (usually natural gas) for the combustion process during discharging and simple cycle modes. In other words, the released air from the cavern should be combined with external fuel in the combustion chamber to enable the turbine [42]. Also, in simple cycle mode, CAES operates as a diesel generator and requires external fuel to operate. Therefore, the emission pollution by the CAES facility during discharging and simple cycle modes are represented by third and fourth terms of (2), respectively. The power and heating purchased from the corresponding market lead to emission pollution. Therefore, the two last terms of the objective function (2) deal with emission pollution, caused by power and heat purchased.

The sets of constraints related to multiple technologies in CHP-based RMG, as well as network constraints, are represented in the following.

2.2. MT constraints

Constraints of MTs optimal scheme are expressed by (3) -(12). Constraints (3) and (4) represent the active and reactive power output limits. The ramp-up and ramp-down rates for continuous times are given in (5) and (6), respectively. Constraints (7)-(10) are related to the minimum up and downtime limits [43]. The start-up and shut-down cost limits are respectively established by (11) and (12).

$$P_i^{\min} I_{i,t} \le P_{i,t,s} \le P_i^{\max} I_{i,t} \tag{3}$$

$$Q_i^{\min} I_{i,t} \le Q_{i,t,s} \le Q_i^{\max} I_{i,t} \tag{4}$$

$$P_{i,t,s} - P_{i,t-1,s} \le R_i^{up} \tag{5}$$

$$P_{i,t-1,s} - P_{i,t,s} \le R_g^{dn} \tag{6}$$

$$I_{i,t} - I_{i,t-1} \le I_{i,t+TU_{i,u}} \tag{7}$$

$$TU_{i,u} = \begin{cases} u & u \le MUT_i \\ 0 & u > MUT_i \end{cases} \tag{8}$$

$$I_{i,t-1} - I_{i,t} \le 1 - I_{i,t+TD_{i,u}} \tag{9}$$

$$TD_{i,u} = \begin{cases} u & u \le MDT_i \\ 0 & u > MDT_i \end{cases} \tag{10}$$

$$\begin{aligned} & SU_{i,t} \ge SUC_i (I_{i,t} - I_{i,t-1}) \\ & SU_{i,t} \ge 0 \end{aligned} \tag{11}$$

$$\begin{aligned} & SD_{i,t} \ge SDC_i (I_{i,t-1} - I_{i,t}) \\ & SD_{i,t} \ge 0 \end{aligned} \tag{12}$$

2.3. CHP unit limitations

Constraints of the CHP unit operation are given by (13) -(23). The CHP operation is realized by a feasible operation region that provides a link between the power and heat output, as depicted in Fig. 2.

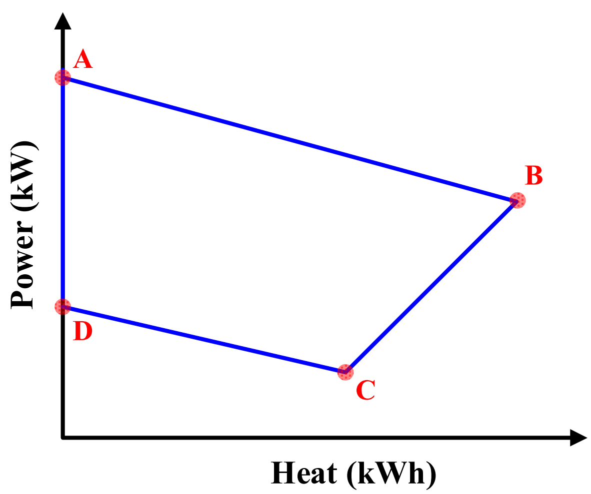

Fig. 2. Power and heat feasible region for the convex CHP operation.

There are four boundary points to determine the generated electricity and heating energy value by CHP. Constraints (13) -(17) determine the relationship between generated heating and power based on the four boundary points. The ramp-up and ramp-down limits are given in (18) and (19), respectively. Equations (20) -(23) show the minimum up and down-time limitations for CHP.

$$P^{chp,min} I_t^{chp} \le P_{t,s}^{chp} \le P^{chp,max} I_t^{chp} \tag{13}$$

$$P_{t,s}^{chp} - P^{chp,A} - \frac{P^{chp,A} - P^{chp,B}}{H^{chp,A} - H^{chp,B}} \times (H_{t,s}^{chp} - H^{chp,A}) \le 0 \tag{14}$$

$$P_{t,s}^{chp} - P^{chp,B} - \frac{P^{chp,B} - P^{chp,C}}{H^{chp,B} - H^{chp,C}} \times H_{t,s}^{chp} - H^{chp,B}) \ge -(1 - I_t^{chp}) \times M \tag{15}$$

$$P_{t,s}^{chp} - P^{chp,C} - \frac{P^{chp,C} - P^{chp,D}}{H^{chp,C} - H^{chp,D}} \times H_{t,s}^{chp} - H^{chp,C}) \ge -(1 - I_t^{chp}) \times M \tag{16}$$

$$0 \le H_{t,s}^{chp} \le H^{chp,A} \times I_t^{chp} \tag{17}$$

$$P_{t,s}^{chp} - P_{t-1,s}^{chp} \le R^{chp,Up} \tag{18}$$

$$P_{t,s}^{chp} - P_{t-1,s}^{chp} \le R^{chp,Dn} \tag{19}$$

$$I_t^{chp} - I_{t-1}^{chp} \le I_{t+UT_{chp,u}}^{chp} \tag{20}$$

$$UT_u^{chp} = \begin{cases} u & u \le T^{chp,on} \\ 0 & u > T^{chp,on} \end{cases} \tag{21}$$

$$I_{t-1}^{chp} - I_t^{chp} \le 1 - I_{t+DT_{chp,u}}^{chp} \tag{22}$$

$$DT_u^{chp} = \begin{cases} u & u \le T^{chp,off} \\ 0 & u > T^{chp,off} \end{cases} \tag{23}$$

2.4. CAES constraints

The proposed RMG is integrated with CAES that can operate in three operation modes: charging, discharging, and simple cycle modes. The simple-cycle process is the starting point for a natural-gas-fired plant. Clean-burning natural gas powers a combustion turbine, which is connected directly to a generator that produces electricity that can operate as a micro-turbine. Sometimes during the operation of CAES, the air cavern is depleted. In order not to disrupt the network, the CAEE must deliver the amount of power to the network. As it is not possible to discharge to the CAES, it operates in the simple cycle mode to generate electricity as a micro-turbine. The restrictions of the CAES scheme are given in (24) -(31). The logical constraint that separates the CAES operation mode at each time is represented by (24). The charging, discharging, and power output in simple cycle modes are bounded by the maximum values that are respectively represented by (25)-(27). The energy capacity of CAES is limited as expressed in (28). Equation (29) realizes the equality condition for the final and initial energy levels. The current available energy capacity of CAES is calculated in (30) [42]. During discharging and simple cycle modes, reactive power is produced by the CAES. Hence, the power output by the CAES is limited by (31).

$$u_{t,s}^{ch} + u_{t,s}^{dis} + u_{t,s}^{sc} \le 1 \tag{24}$$

$$0 \le P_{t,s}^{ch} \le P^{ch,\max} u_{t,s}^{ch} \tag{25}$$

$$0 \le P_{t,s}^{dis} \le P^{dis,\max} u_{t,s}^{dis} \tag{26}$$

$$0 \le P_{t,s}^{sc} \le P^{sc,\max} u_{t,s}^{sc} \tag{27}$$

$$E^{\min} \le E_{t,s} \le E^{\max} \tag{28}$$

$$E_{t=0,s} = E_{\text{int}} \tag{29}$$

$$E_{t,s} = E_{t-1,s} + P_{t,s}^{ch} - P_{t,s}^{dis} \times ER \tag{30}$$

$$\left(P_{t,s}^{dis} + P_{t,s}^{sc}\right)^2 + \left(Q_{t,s}^{\exp}\right)^2 \le \left(S_{\max}^{\exp}\right)^2 \tag{31}$$

2.5. TES constraints

The fast-growing of the multi-carrier energy system provides a suitable opportunity to develop TES in the energy system for achieving multiple economic and environmental benefits [44]. The logical constraint for the TES operation is expressed in (32). Equations (33) and (34) signify the min and max limits of discharged and charged heating values, respectively. Equation (35) determines the heating capacity. The heating capacity limit is represented in (36). Equation (37) realizes the equality condition for the final and initial energy levels of TES.

$$Ih_{t,s}^{D} + Ih_{t,s}^{CH} \leq 1 \tag{32}$$

$$H^{D,\min} Ih_{t,s}^{D} \leq H_{t,s}^{D} \leq H^{D,\max} Ih_{t,s}^{D} \tag{33}$$

$$H^{CH,\min} Ih_{t,s}^{CH} \leq H_{t,s}^{CH} \leq H^{CH,\max} Ih_{t,s}^{CH} \tag{34}$$

$$HS_{t,s} = HS_{t\text{-}1,s}(1-eh) + eh^{CH} H_{t,s}^{CH} - \frac{H_{t,s}^{D}}{eh^{D}} \tag{35}$$

$$HS^{\min} \leq HS_{t,s} \leq HS^{\max} \tag{36}$$

$$HS_{t=0,s} = HS_{t=24,s} \tag{37}$$

2.6. DRP constraints

As previously discussed, the shiftable loads are considered in RMG's model. Based on the time activity of multiple loads, the RMG operator can schedule the responsible loads. Equation (38) expresses the amount of load after the DRP. The total value of load interruption at any period should be compensated at other hours as established in (39). The load value that participates in DRP is limited by (40). The maximum allowable load that participates in DRP is determined in (41). The LPF factor denotes the load participating factor in DRP. There are several types of consumers in the system. However, only a percentage of the system load participates in the DRP.

In this paper, 10% of the load participates in the DRP, hence the LPF equals 0.1. Constraint (42) expresses the active and reactive responsible loads relationship.

$$D_{l,t,s}^{DR} = D_{l,t,s} + DR_{l,t,s} \tag{38}$$

$$\sum_{t} DR_{l,t,s} = 0 \tag{39}$$

$$\left| DR_{l,t,s} \right| \le DR_{l,t,s}^{\max} \tag{40}$$

$$DR_{l,t,s}^{\max} = LPF \; D_{l,t,s} \tag{41}$$

$$Q_{l,t,s}^{DR} = \tan\phi \; D_{l,t,s}^{DR} \tag{42}$$

2.7. Wind power generation constraint

The power produced by the wind unit depends on the hourly wind speed. The power generated by the wind unit is calculated by (43). Equation (44) shows the active and reactive power limits of the wind turbine. The value of wind power curtailment shouldn't exceed the hourly wind power output in each scenario.

$$P_{w,t,s} = \begin{cases} 0 & 0 \le \upsilon_{w,t,s} \le \upsilon_{cut-in} \\ \dfrac{\upsilon_{w,t,s} - \upsilon_{cut-in}}{\upsilon_{rated} - \upsilon_{cut-in}} \times P_{w,R} & \upsilon_{cut-in} \le \upsilon_{w,t,s} \le \upsilon_{rated} \\ P_{w,R} & \upsilon_{rated} \le \upsilon_{w,t,s} \le \upsilon_{cut-out} \end{cases} \tag{43}$$

$$(P_{w,t,s}^{f} - P_{w,t,s}^{curt})^2 + (Q_{w,t,s}^{f})^2 \le S_{w}^{2} \tag{44}$$

$$P_{w,t,s}^{curt} \le P_{w,t,s}^{f} \tag{45}$$

2.8. Power flow constraints

As previously discussed, the AC-optimal power flow model is established to model the power flow in the RMG. Active and reactive power balance restrictions are represented by (46) and (47), respectively. It should be noted that the two first terms in (46) and the first term of (47) are only considered for the main bus. The active and reactive power flow in each feeder is calculated by (48) and (49). The thermal capacity limit of the feeder is established by (50). Constraint (51) expresses the voltage limitation on buses.

$$P^{buy}_{t,s} - P^{sell}_{t,s} + \sum_{i=1}^{NU_b}(P_{i,t,s}) + P^{f}_{w,t,s} - P^{curt}_{w,t,s} + P^{sc}_{t,s} + P^{dis}_{t,s} - P^{ch}_{t,s} - \sum_{l=1}^{NL_b} d^{dr}_{l,t,s} - \sum_{L=1}^{NLI_b} PF_{L,t,s} = 0 \tag{46}$$

$$Q^{upstr}_{t,s} + \sum_{i=1}^{NU_b} Q_{i,t,s} + Q^{f}_{w,t,s} + Q^{chp}_{t,s} + Q^{\exp}_{t,s} - \sum_{l=1}^{NL_b} Q^{dr}_{l,t,s} - \sum_{L=1}^{NLI_b} QF_{L,t,s} = 0 \tag{47}$$

$$PF_{L,t,s} = \left(\frac{V^2_{b,t,s}}{Z_{b,b'}} \cos(\theta_{b,b'}) - \frac{V_{b,t,s} V_{b',t,s}}{Z_{b,b'}} \cos(\delta_{b,t,s} - \delta_{b',t,s} + \theta_{b,b'}) \right) \tag{48}$$

$$QF_{L,t,s} = \left(\frac{V^2_{b,t,s}}{Z_{b,b'}} \sin(\theta_{b,b'}) - \frac{V_{b,t,s} V_{b',t,s}}{Z_{b,b'}} \sin(\delta_{b,t,s} - \delta_{b',t,s} + \theta_{b,b'}) \right) \tag{49}$$

$$PF^2_{L,t,s} + QF^2_{L,t,s} \le S^2_L \tag{50}$$

$$V^{\min}_b \le V_{b,t,s} \le V^{\max}_b \tag{51}$$

2.9. Reconfiguration constraints

The reconfiguration modifies the MG structure by changing the switches' status. The reconfiguration capability can transfer the load from heavily loaded parts to lightly ones contributing to power loss reduction. In this way, the maximum utilization of the feeders' capacity is achieved. Two types of switches named normally closed and normally opened (tie-switches) are embedded in the MG. The status of each switch is indicated by a binary variable ($K_{L,t}$). $K_{L,t}$ equals 1 if the switch is closed, being 0 otherwise. Constraint (52) and (53) reformulate the active and reactive power flow considering reconfiguration capability. To guarantee the radiality structure of CHP-based RMG, in each given period, the number of opened switches must be equals to the number of primarily opened switches before applying the reconfiguration process. In other words, no loops should appear in the structure, as established by constraint (54). Constraint (55) satisfies the radiality topology and prevent making any loops.

$$PF_{L,t} = \left(\frac{V_{b,t,s}^{2}}{Z_{b,b'}} \cos(\theta_{b,b'}) - \frac{V_{b,t,s} V_{b',t,s}}{Z_{b,b'}} \cos(\delta_{b,t,s} - \delta_{b',t,s} + \theta_{b,b'}) \right) K_{L,t,s} \tag{52}$$

$$QF_{L,t} = \left(\frac{V_{b,t,s}^{2}}{Z_{b,b'}} \sin(\theta_{b,b'}) - \frac{V_{b,t,s} V_{b',t,s}}{Z_{b,b'}} \sin(\delta_{b,t,s} - \delta_{b',t,s} + \theta_{b,b'}) \right) K_{L,t,s} \tag{53}$$

$$\sum_{L=1}^{NLI_{lp}} K_{L,t,s} = NCS_{lp} \tag{54}$$

$$\sum_{L=1}^{NLI_{lp}} K_{L,t,s} \leq NPL_{lp} - 1 \tag{55}$$

2.10. Thermal balance constraint

The CHP system generates power and heat based on the feasible operating region. Also, the TES is coupled with the CHP system to store the generated heat and enables RMG's operator to sell heating energy to the thermal market. Constraint (56) establishes a thermal balance constraint.

$$H_{t,s}^{D} - H_{t,s}^{CH} + H_{t,s}^{chp} = H_{t,s}^{sell} - H_{t,s}^{buy} \tag{56}$$

3. Solution method

As discussed, the optimal RMG scheduling in the presence of multiple components to minimize operation costs, as well as emission pollution, is formulated as a multi-objective optimization problem. To solve the proposed multi-objective problem, the Ɛ-constraint method is implemented, which is described as following.

It is assumed that there is an optimization problem including k-objectives (that may have a conflict with each other), and corresponding constraints as (57):

$$W = \max\{f_1(x), f_2(x), f_2(x), ..., f_k(x)\}$$

$$\text{Subject to:} \quad x \in A \tag{57}$$

Where A is a feasible region for the multi-objective problem and x is a set of decision variables. In the epsilon-constraint method, one of the objective functions is captured as the basic goal, and others are assigned as its constraints. For example, the multi-objective problem (57) is transferred to (58) based on the epsilon- constraint:

$$\begin{aligned} & W = \max f_1(x) \\ & \text{Subject to:} \\ & \quad f_2(x) \geq \varepsilon_2 \\ & \quad f_3(x) \geq \varepsilon_3 \\ & \quad \vdots \\ & \quad f_k(x) \geq \varepsilon_k \\ & \quad x \in A \end{aligned} \tag{58}$$

The members of Ɛ-set: $\{\varepsilon_2, \varepsilon_3, \varepsilon_4, ..., \varepsilon_k\}$, are modified parametrically to find the most optimum solutions. The optimum solution values of Ɛ-set are determined based on the *k-1* objective functions.

There are various methods to find the optimal solution among the generated Pareto set in the multi-objective optimization problem. The fuzzy-based decision-making approach is one of the best solutions to find the optimum solutions among all solutions in the Pareto set. In this approach, for all available solutions in the Pareto set, the membership function $\in [0,1]$ is assigned. The membership function shows the degree of optimally for all objective functions of the k^{th} Pareto solution. For each of the objective function in (57), the fuzzy membership is calculated as follows:

$$\hat{f}_k = \begin{cases} 1 & f_k \le f_k^{L} \\ \dfrac{f_k^{\max} - f_k}{f_k^{\max} - f_k^{\min}} & f_k^{L} \le f_k \le f_k^{u} \\ 0 & f_k \ge f_k^{u} \end{cases} \tag{59}$$

To specify the best reconciliation between produced solutions, the min-max method based on the minimum values of f_1 and f_2, and selecting the maximum optimum of $\left[\min\left\{\hat{f}_1,\hat{f}_2\right\}\right]$ is applied.

Fig. 3 shows the flowchart of the proposed multi-objective operation of renewable and CHP-based RMG with multiple components to minimize operational cost and emission, which is solved by Ɛ-constraint and fuzzy-based decision-making method.

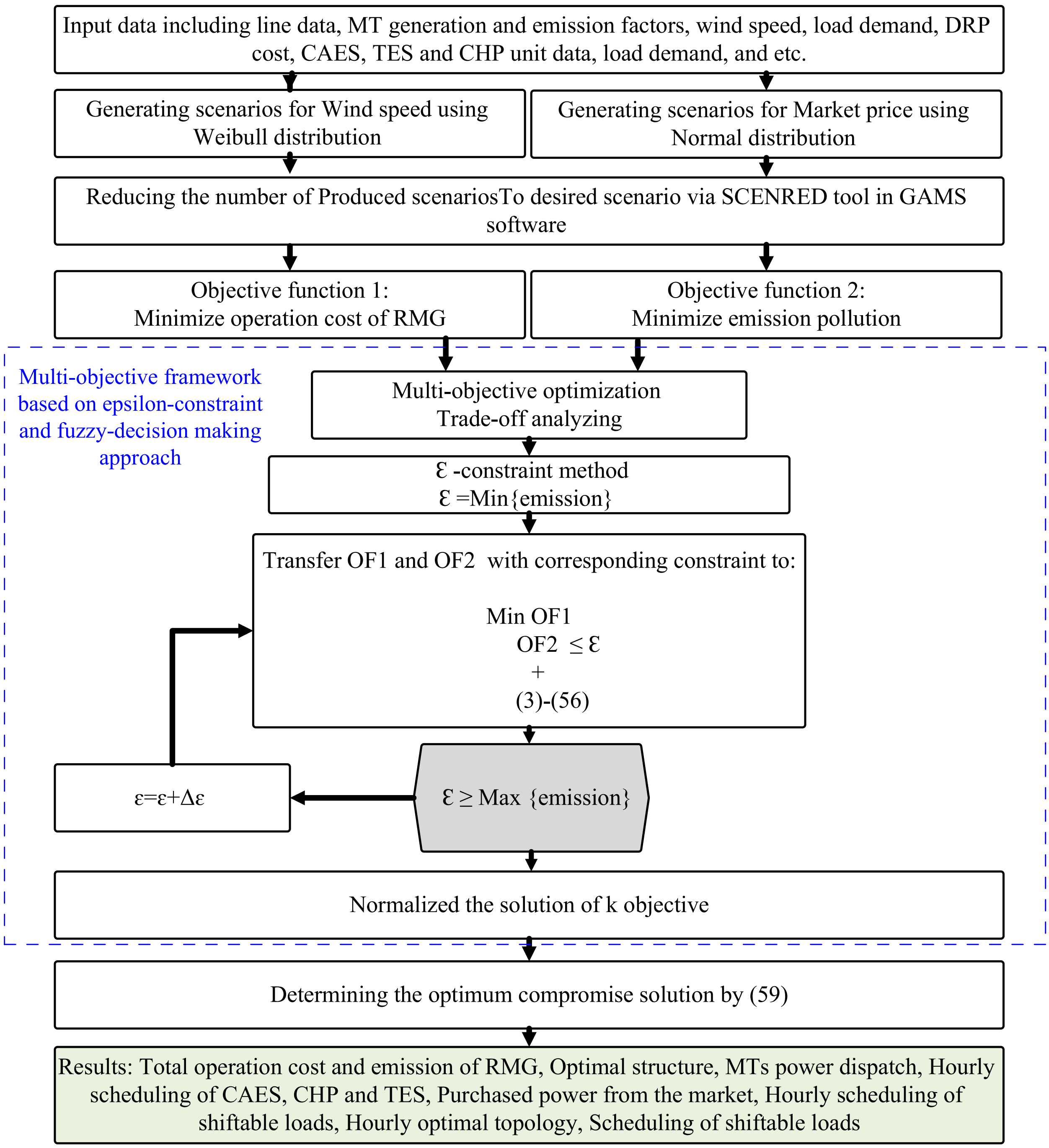

Fig. 3. The flowchart of the solution method for the proposed multi-objective problem.

4. Simulation Results

4.1. Case study

The proposed multi-objective CHP-based RMG model, equipped with multiple components, is examined on the sampled 10-bus microgrid, which is depicted in Fig. 4. The forecasted load demand (active and reactive) with wind power output is depicted in Fig. 5. The daily power and thermal prices are shown in Fig. 6. All the characteristics of MTs (G1 and G2) and CHP units are presented in [34, 45]. The maximum charge, discharge, and simple cycle value of the CAES facility are 20 kW, and the maximum capacity of the cavern is 100 kWh. Other characteristics of the CAES facility are given in [20]. The maximum capacity and charge and discharge values of TES are 20 kW, 20 kW, and 100 kWh, respectively. The natural gas price is assumed to be constant during the time horizon and equal to 1.8 ¢/Mbtu. Also, the cost of demand response is considered 5 ¢/kWh.

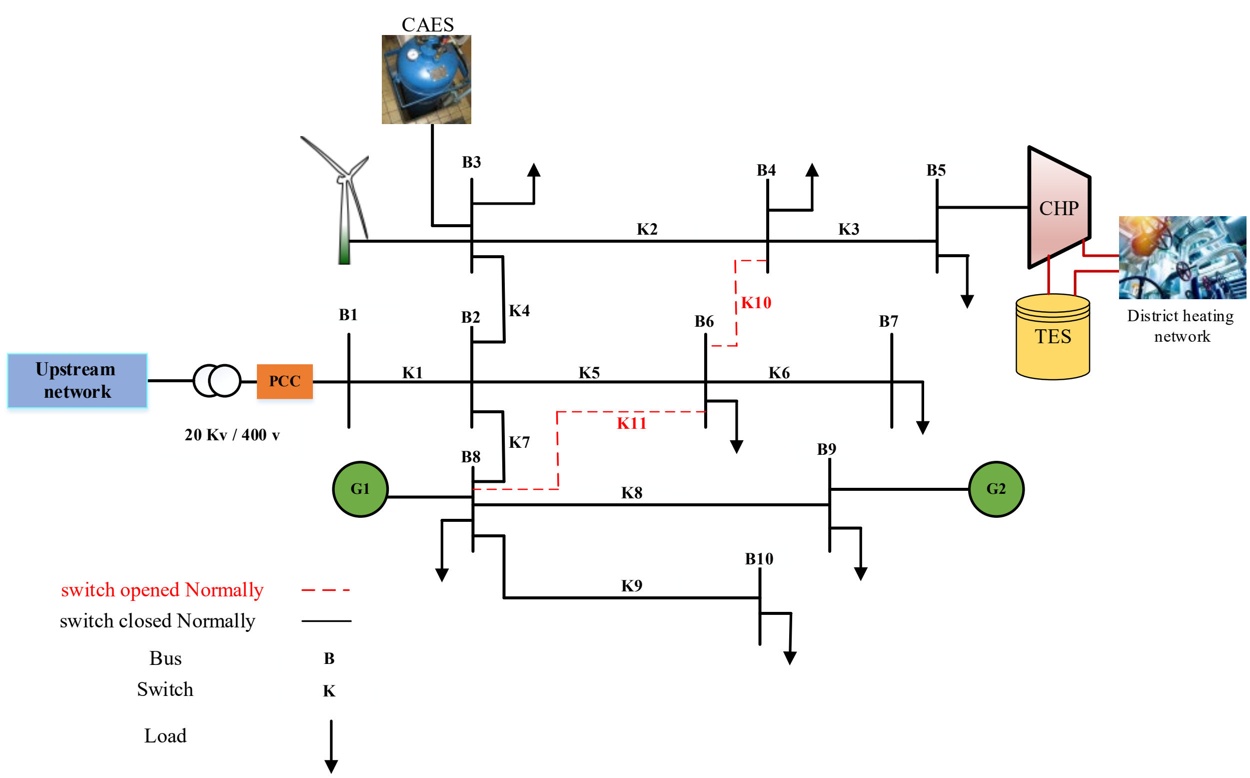

Fig. 4. The sampled 10-bus reconfigurable microgrid with multiple components.

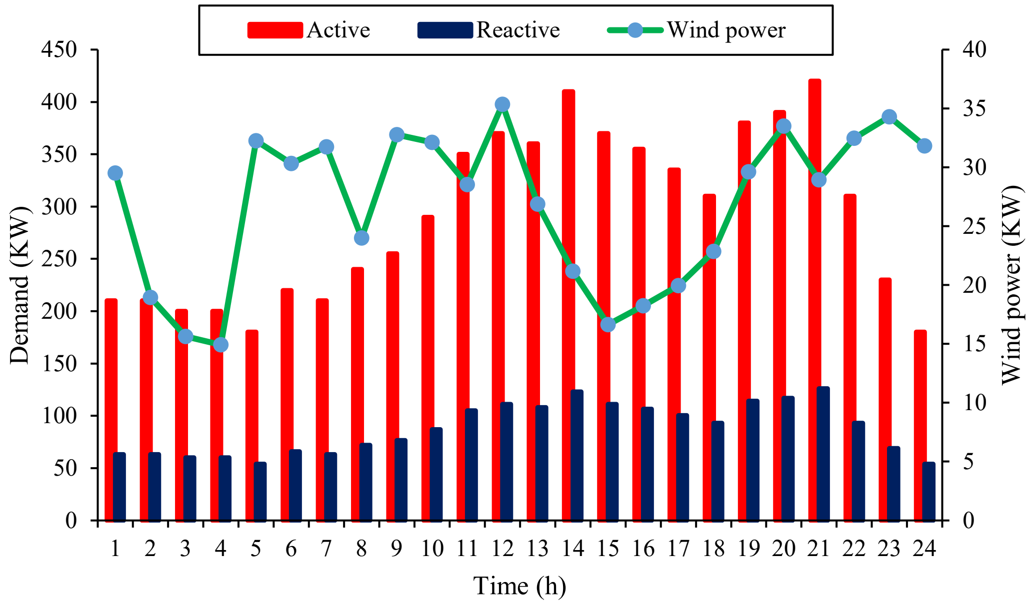

Fig. 5. The forecasted load demand and wind power generation.

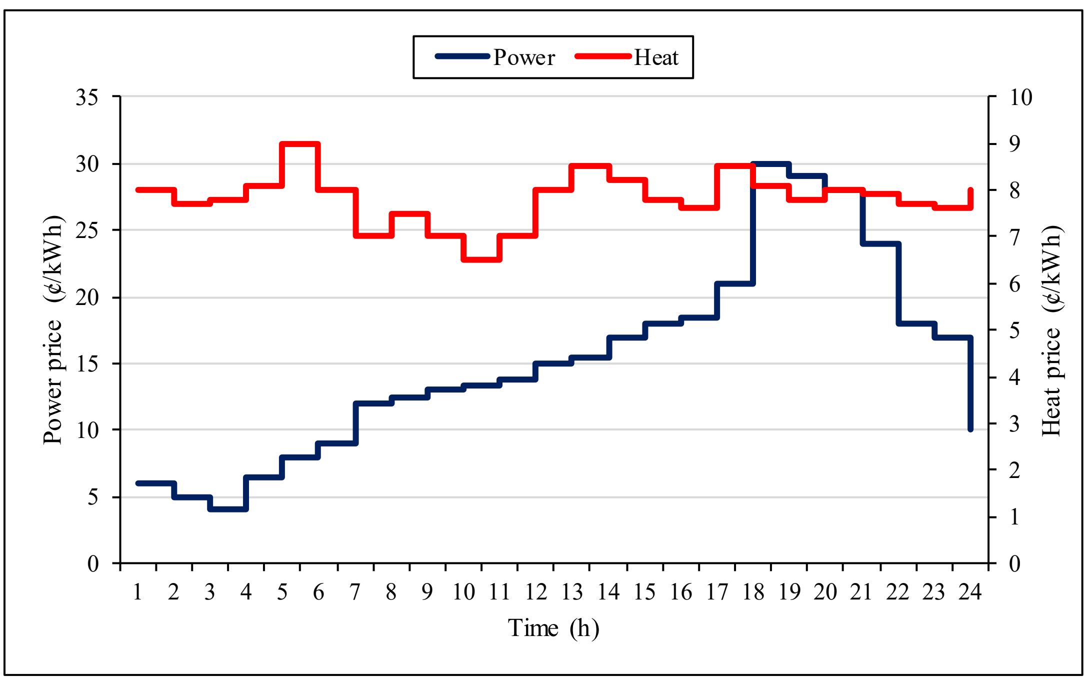

Fig. 6. The hourly power and heat prices.

4.2. Numerical results

The proposed multi-objective problem was formulated as an MINLP model carried out in GAMS software and solved by a DICOPT solver. To model uncertainties caused by electricity power price and wind power production, 1000 scenarios are produced using the Monte-Carlo simulation that is reduced to 10 most likely scenarios using the SCENRED tool in GAMS software. It should be noted that the forecasted errors of wind power and electricity price follow the Weibull and Normal distribution function, respectively [46].

Numerical results are provided for two cases. At first, the optimal operation of the CHP-based RMG is solved as a single objective model to minimize operational cost. Then, the multi-objective two-stage optimization model of the CHP-based RMG to minimize emission and operational cost is extended.

The probability and corresponding operational cost of each scenario are indicated in Table II. Hence, the expected value of the total operation cost is $90164.65.

Table II. The operation cost and probability value for reduced scenarios

Scenarios	*S1*	*S2*	*S3*	*S4*	*S5*	*S6*	*S7*	*S8*	*S9*	*S10*
Scenarios probability	0.153	0.047	0.109	0.002	0.002	0.021	0.158	0.252	0.154	0.102
Operation cost (¢)	89413.626	78085.459	91846.177	94553.085	92693.746	90760.152	90292.785	85408.517	87257.926	74309.178

To demonstrate the effects of the proposed model, the following cases are examined:

1. Evaluating the optimal scheduling of RMG under a single-objective model.
2. Evaluating the optimal scheduling of RMG considering economic and environmental goals based on the multi-objective framework.

According to Table II, scenario number 8 has the highest probability. Hence, this scenario is selected to show the results, including power dispatch, CAES scheme, DRP effects, hourly reconfiguration, etc. in detail.

- **Evaluating the power dispatch in Case 1**

The optimal power dispatch of the local generation resources, as well as the hourly power exchanged with the upstream network for scenario number 8, is given in Fig. 7. For the periods 12-23 (higher load demand hours), the CHP unit is committed to producing power with the maximum capacity. The G1 is committed for periods between 13 to 23 to satisfy economic benefits, while the G2 as the expensive generation unit, is only committed between hours 14-22 when the load demand reaches a higher value. Furthermore, as shown in Fig. 6, when the electricity price is low, the RMG operator tends to purchase more power from the upstream grid. As the electricity prices reach higher values, the power purchased from the grid is reduced. For the periods 18-20, as the electricity price is higher than other periods, the operator tends to sell extra power generated by local resources to the upstream network and contributes to more economic savings benefits.

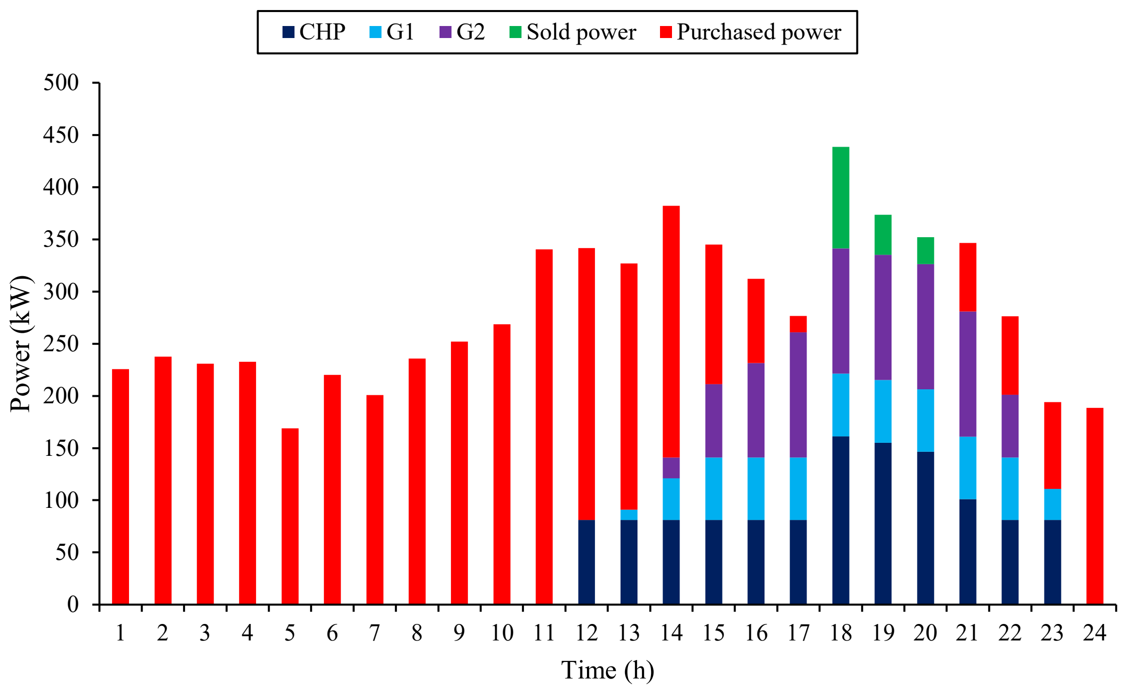

Fig. 7. Hourly power dispatch by units and power exchanged with the main grid in scenario 8.

- **Evaluating the optimal scheduling of CAES in Case 1**

The optimal scheme of the CAES facility for scenario number 8 is given in Fig. 8. According to Fig. 8, for periods 1-4, as the electricity price is lower than other hours, the CAES is charged. Then, for the periods, including 13, 17-18, and 22, the CAES is discharged and injects the power to the MG. Also, for the periods, including 14-16, 19-21, and 23, CAES operates in the simple-cycle mode and generates electricity to meet local demand. The main reasons for this phenomenon are related to the higher electricity price compared with natural gas price, as well as the operation cost of CAES in simple-cycle mode compared to discharged mode. Therefore, at these periods, CAES operates as a conventional diesel generator and generates power to satisfy more economic benefits.

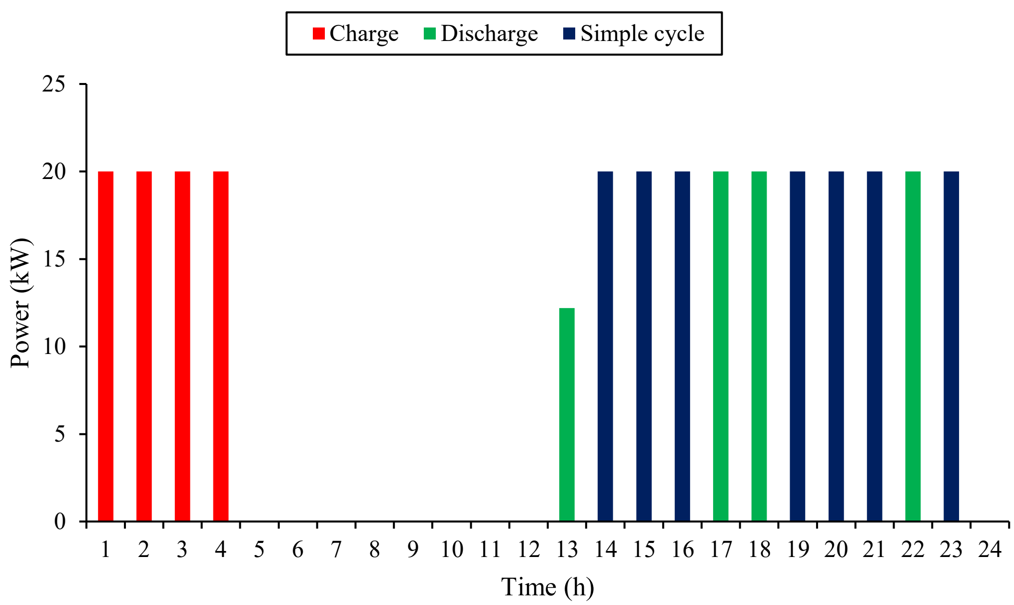

Fig. 8. The optimal scheme of CAES facility for scenario number 8.

- **Evaluating the thermal energy procedure**

The optimal scheme of TES, as well as the generated heat by the CHP unit for scenario number 8, are depicted in Fig. 9. According to Fig. 9, at lower heat prices, the TES is charged. As the heat prices reach higher values, TES is discharged. Also, due to the feasible operation region and the interdependency between produced electricity and heating energy by the CHP, as it is committed to producing electricity, the heating energy is generated. Therefore, the coordinated scheme between the CHP unit and TES provides an opportunity for the operator to participate in the thermal market and saving costs.

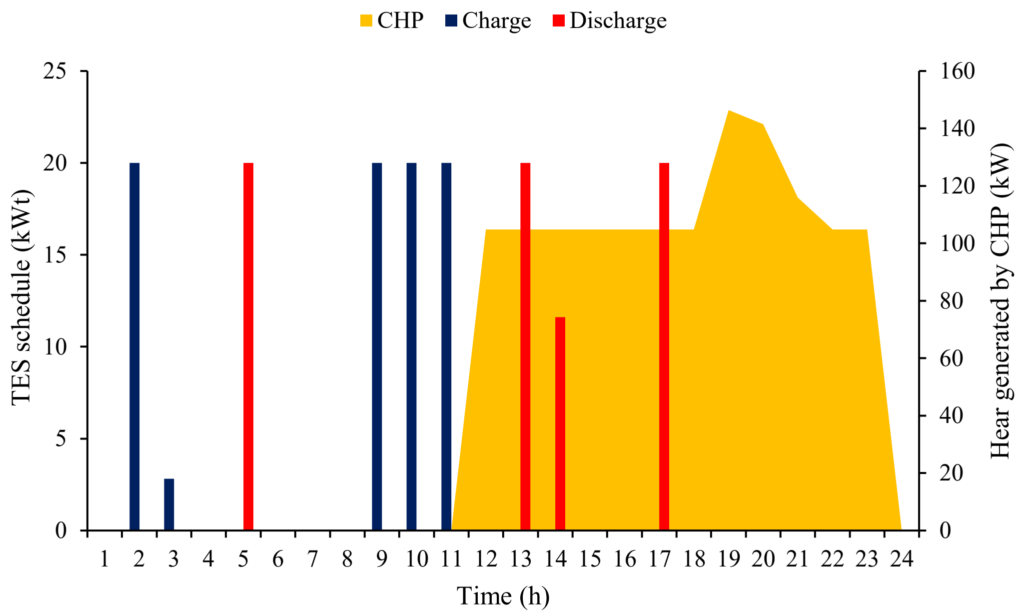

Fig. 9. The hourly charging-discharging scheme of TES and generated heat by CHP unit for scenario 8.

- **Evaluating the DRP on the load profile in Case 1**

The effect of the DRP on the hourly load profile for scenario number 8 is depicted in Fig. 10. According to Fig. 10, the load demand shifts from higher electricity price hours to lower electricity prices times through DRP execution. For the first hours of the day, when the electricity is lower than in other periods, the load profile is increased. For the higher demand hours (16-23), the operator encourages the responsible load to reduce their demand. Consequently, the load profile peak is shifted. Increasing and decreasing load value during off-peak intervals, and peak hours, respectively, while smoothes the load profile compared with the initial load profile, provides an appropriate solution for more cost-saving.

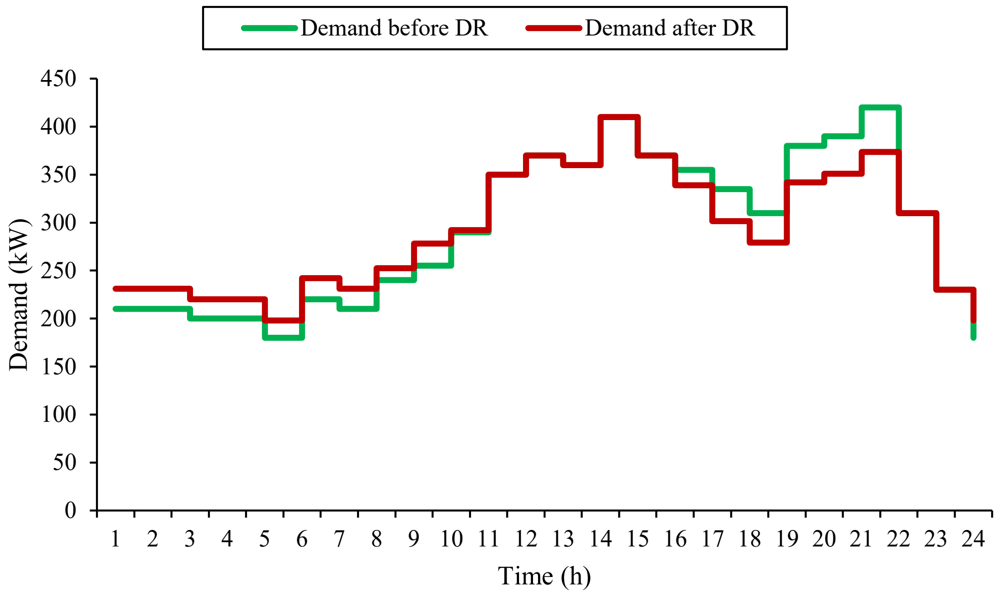

Fig. 10. The effect of DRP on the network load profile.

- **Evaluating the effect of reconfiguration capability**

The optimal hourly topology of the RMG in scenario number 8 is given in Table III. As previously discussed, reconfiguration uses the maximum of the feeder's capacity by transferring the load from heavily loaded parts to lightly ones. As can be seen from Table III, there are two open switches in the RMG's topology at each period. The optimal scheduling of the network switches results in minimizing the RMG power loss, which contributes towards a lower operating cost.

Table III. The optimal hourly switches status through reconfiguration.

Time (h)	***K1***	***K2***	***K3***	***K4***	***K5***	***K6***	***K7***	***K8***	***K9***	***K10***	***K11***
1	✓	✓	✓	✓	✓	✓	✓	✓	✓	×	×
2	✓	✓	✓	✓	✓	✓	✓	✓	✓	×	×
3	✓	×	✓	✓	✓	✓	✓	✓	✓	✓	×
4	✓	×	✓	✓	✓	✓	✓	✓	✓	✓	×
5	✓	×	✓	✓	✓	✓	✓	✓	✓	✓	×
6	✓	×	✓	✓	✓	✓	✓	✓	✓	✓	×
7	✓	×	✓	✓	✓	✓	✓	✓	✓	✓	×
8	✓	×	✓	✓	✓	✓	✓	✓	✓	✓	×
9	✓	✓	✓	✓	✓	✓	✓	✓	✓	×	×
10	✓	✓	✓	✓	✓	✓	✓	✓	✓	×	×
11	✓	✓	✓	✓	✓	✓	✓	✓	✓	×	×
12	✓	✓	✓	✓	✓	✓	✓	✓	✓	×	×

13	✓	✓	✓	✓	✓	✓	✓	✓	✓	×	×
14	✓	✓	✓	✓	✓	✓	✓	✓	✓	×	×
15	✓	✓	✓	✓	✓	✓	×	✓	✓	×	✓
16	✓	×	✓	✓	✓	✓	×	✓	✓	✓	✓
17	✓	×	✓	✓	✓	✓	✓	✓	✓	✓	×
18	✓	×	✓	✓	✓	✓	×	✓	✓	✓	✓
19	✓	✓	✓	✓	✓	✓	×	✓	✓	×	✓
20	✓	×	✓	✓	✓	✓	×	✓	✓	✓	✓
21	✓	×	✓	✓	✓	✓	×	✓	✓	✓	✓
22	✓	✓	✓	✓	✓	✓	×	✓	✓	×	✓
23	✓	✓	✓	✓	✓	✓	×	✓	✓	×	✓
24	✓	×	✓	✓	✓	✓	✓	✓	✓	✓	×

The simultaneous effect of reconfigurable capability along with the CAES, TES, and DRP on the total expected cost and active power losses are represented in Table IV. According to Table IV, considering reconfigurable capability, CAES, TES, and DRP simultaneously, the total operation cost reduced up to 3 %. Also, reconfigurable capability plays a major role in reducing the active power loss of up to 10.28%.

Table IV. Simultaneous effect of multiple resources on the expected operation cost, and power loss.

	-	*CAES*	*CAES+TES*	*CAES+TES+DR*	*CAES+TES+DR+ reconfiguration capability*
Expected operation cost (¢)	94513.417	93112.187	92866.900	90766.465	90162.964
Expected power losses (kWh)	145.6	144.3	144.3	155.6	139.6

Case 2:

The proposed results in the previous part are related to the single-objective optimization framework, while the emission pollution is neglected. Now, the multi-objective is solved to minimize the operational cost, as well as environmental pollution.

Pareto solutions for the multi-objective problem in the presence of all the sources are listed in Table V for 10 iterations. According to Table V, as the environmental benefit reduces, the operation cost of the RMG increases. This action indicates a conflict between the operational cost and the emission benefits. After the implementation of the fuzzy-based decision-making approach, and are normalized, and the maximum value between all minimum values are selected. Iteration numbers 2 and 6 are selected to analyze the optimal multi-objective scheduling of the RMG in detail.

Table V. The optimal Pareto solutions for the proposed multi-objective problem.

Iteration	Expected operation cost (¢)	Expected emission (kgco2/day)	$\hat{f}_1$	$\hat{f}_2$
1	90162.964	5820.047	1	0
2	90708.273	5653.472	0.977	0.023
3	90751.219	5486.897	0.976	0.024
4	91461.124	5320.322	0.947	0.053
5	92880.674	5153.747	0.889	0.111
6	94848.866	4987.172	0.809	0.191
7	**97449.057**	**4820.597**	**0.652**	**0.348**
8	101950.468	4654.022	0.329	0.671
9	106302.947	4487.447	0.342	0.888
10	114710.359	4320.872	0	1

- **Evaluating the optimal scheduling of CAES in Case 2**

The optimal power dispatch of local generation units, including G1, G2, and CHP for iteration numbers 2 and 6 are compared in Fig. 11. According to Fig. 11, the values of total power dispatch by all units (especially G1 and G2) are significantly increased, which increases the operational cost, and consequently, reducing the emission pollution.

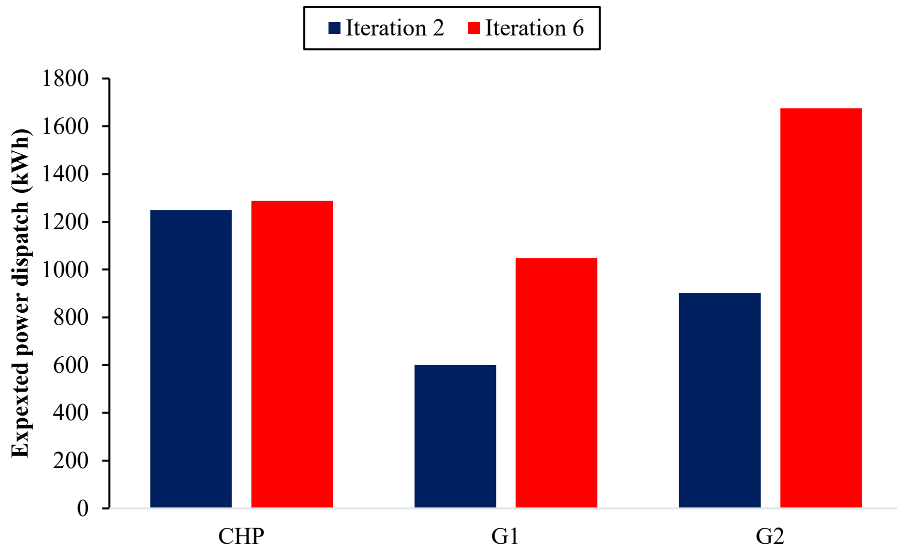

Fig. 11. The effect of pollution reduction on the power generation for two iterations.

- **Evaluating the optimal exchanged for Case 2**

The hourly power exchanged between the main grid and RMG for iterations numbers 2 and 6 is drawn in Fig. 12. The power purchased has a significant impact on total emission pollution. Hence, in iteration number 6, as the total operational cost increases, the operator tends to decreases the power exchanged with the upstream network, results in emission pollution reduction.

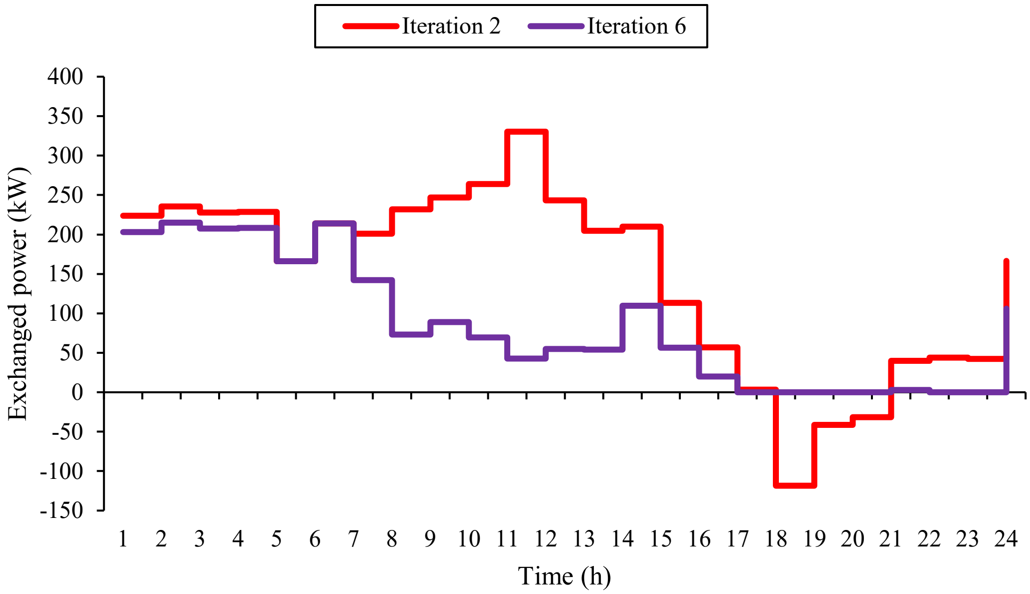

Fig. 12. The effect of pollutant gas production reduction on the microgrid power exchange

- **Evaluating the optimal scheme of CAES and TES in Case 2**

The optimal scheme of CAES and TES for iteration number 2 and 6 are shown in Table VI. In iteration number 6, the value of the charge and discharge scheme for the TES is significantly reduced. Also, the CAES is mainly operated in a simple cycle mode. The heating exchanged with the thermal market decreases, and TES is less utilized in iteration number 6. Also, by operating in the simple-cycle mode in iteration number 6, the CAES facility releases less carbon dioxide. Consequently, the environmental benefit is satisfied.

Table VI. Energy distribution of CAES and TES for two different iterations.

	TES				***CAES***					
	Iteration 2		***Iteration 6***		***Iteration 2***			***Iteration 6***		
	Charge mode	Discharge mode	Charge mode	Discharge mode	Charge mode	Discharge mode	Simple cycle mode	Charge mode	Discharge mode	Simple cycle mode
Power (kWh)	82.81	71.606	20	17.691	80	72.2	160	0	0	340

- **Evaluating the reconfiguration capability in Case 2**

The four switches status with the most changes in the hourly topology of RMG in iteration number 2 and 6 for scenario number 8 are given in Table VII. As can be seen, the optimal hourly switch status for two iterations are different. The optimal switches status in iteration number 6 is to reduce the total emission pollution.

Table VII. The optimal scheduling of the reconfiguration process for two different iterations.

Time (h)	*Iteration 2*				*Iteration 6*			
	K2	*K7*	*K10*	*K11*	*K2*	*K7*	*K10*	*K11*
1	✓	✓	×	×	✓	✓	×	×
2	✓	✓	×	×	✓	✓	×	×
3	×	✓	✓	×	×	✓	✓	×
4	×	✓	✓	×	×	✓	✓	×
5	×	✓	✓	×	×	✓	✓	×
6	×	✓	✓	×	×	✓	✓	×
7	×	✓	✓	×	×	✓	✓	×
8	×	✓	✓	×	×	×	✓	✓
9	✓	✓	×	×	×	×	✓	✓
10	✓	✓	×	×	×	×	✓	✓
11	✓	✓	×	×	✓	✓	×	×
12	✓	✓	×	×	×	×	✓	✓
13	✓	✓	×	×	×	×	✓	✓
14	✓	✓	×	×	×	×	✓	✓
15	✓	×	×	✓	×	×	✓	✓
16	×	×	✓	✓	✓	✓	×	×
17	×	✓	✓	×	✓	×	×	✓
18	×	×	✓	✓	×	×	✓	✓
19	✓	×	×	✓	✓	✓	×	×
20	×	×	✓	✓	✓	✓	×	×
21	×	×	✓	✓	×	×	✓	✓
22	✓	×	×	✓	×	✓	✓	×
23	✓	×	×	✓	×	×	✓	✓
24	×	✓	✓	×	×	✓	✓	×

5. Conclusion

The optimal two-stage multi-objective scheduling of the combined heat and power-based reconfigurable microgrid integrated with demand response program, compressed air energy storage, thermal energy storage, and wind energy was proposed in this paper, which considers the reconfiguration capability. The operator optimized the operation of multiple components, as well as power and heating, exchanged (selling or purchasing) with electricity and thermal markets, considering the AC-power flow equation to minimize total operational cost and emission pollution. By considering wind power, and electricity price variability, the proposed model was formulated as multi-objective two-stage stochastic programming, and the ε-constraint approach was used to solve the problem. The proposed model was examined on a reconfigurable microgrid test system, and numerical results were discussed for different cases. The following major conclusions are drawn from the results:

- The integration of multiple energy storage systems consists of CAES, and TES reduces the total operational cost up to 1%.
- The integration of demand response programs in the model reduces the total operational cost up to 2.26%.
- For more emission reduction, the CAES facility is only operated in simple-cycle mode, and the charge/ discharge scheme of TES is mainly reduced. Also, the power exchanged between RMG and the upstream grid is reduced to satisfy environmental benefits.
- Reconfiguration capability transfers the load from heavily loaded sections to lightly ones, contributing to the power loss reduction of up to 10%.
- Simultaneously integration of all flexible resources, including CAES, TES, reconfiguration capability, and demand response, reduce total operational cost and emission up to 3% and 10.28%, respectively.

Reference

[1] S. G. M. Rokni, M. Radmehr, and A. Zakariazadeh, "Optimum energy resource scheduling in a microgrid using a distributed algorithm framework," *Sustainable cities and society,* vol. 37, pp. 222-231, 2018.

[2] P. G. Panah, R.-A. Hooshmand, and M. Gholipour, "A techno-economic analysis: Urban reconfigurable microgrids participating in short-term regulating power markets," *Sustainable Cities and Society,* p. 102181, 2020.

[3] B. Llamas, C. Laín, M. C. Castañeda, and J. Pous, "Mini-CAES as a reliable and novel approach to storing renewable energy in salt domes," *Energy,* vol. 144, pp. 482-489, 2018.

[4] R. Jabbari-Sabet, S.-M. Moghaddas-Tafreshi, and S.-S. Mirhoseini, "Microgrid operation and management using probabilistic reconfiguration and unit commitment," *International Journal of Electrical Power & Energy Systems,* vol. 75, pp. 328-336, 2016.

[5] G. Cardoso, M. Stadler, A. Siddiqui, C. Marnay, N. DeForest, A. Barbosa-Póvoa*, et al.*, "Microgrid reliability modeling and battery scheduling using stochastic linear programming," *Electric power systems research,* vol. 103, pp. 61-69, 2013.

[6] Z. Shi, H. Liang, S. Huang, and V. Dinavahi, "Distributionally robust chance-constrained energy management for islanded microgrids," *IEEE Transactions on Smart Grid,* vol. 10, pp. 2234-2244, 2018.

[7] Z. Li and Y. Xu, "Optimal coordinated energy dispatch of a multi-energy microgrid in grid-connected and islanded modes," *Applied Energy,* vol. 210, pp. 974-986, 2018.

[8] A. M. Haidar, A. Fakhar, and A. Helwig, "Sustainable energy planning for cost minimization of autonomous hybrid microgrid using combined multi-objective optimization algorithm," *Sustainable Cities and Society,* p. 102391, 2020.

[9] L. Wang, Q. Li, R. Ding, M. Sun, and G. Wang, "Integrated scheduling of energy supply and demand in microgrids under uncertainty: A robust multi-objective optimization approach," *Energy,* vol. 130, pp. 1-14, 2017.

[10] M. Hemmati, B. Mohammadi-Ivatloo, M. Abapour, and A. Anvari-Moghaddam, "Optimal Chance-Constrained Scheduling of Reconfigurable Microgrids Considering Islanding Operation Constraints," *IEEE Systems Journal,* 2020.

[11] L. Ma, N. Liu, J. Zhang, W. Tushar, and C. Yuen, "Energy management for joint operation of CHP and PV prosumers inside a grid-connected microgrid: A game theoretic approach," *IEEE Transactions on Industrial Informatics,* vol. 12, pp. 1930-1942, 2016.

[12] M. Sedighizadeh, M. Esmaili, and N. Mohammadkhani, "Stochastic multi-objective energy management in residential microgrids with combined cooling, heating, and power units considering battery energy storage systems and plug-in hybrid electric vehicles," *Journal of Cleaner Production,* vol. 195, pp. 301-317, 2018.

[13] Z. Luo, Z. Wu, Z. Li, H. Cai, B. Li, and W. Gu, "A two-stage optimization and control for CCHP microgrid energy management," *Applied Thermal Engineering,* vol. 125, pp. 513-522, 2017.

[14] F. Nazari-Heris, B. Mohammadi-ivatloo, and D. Nazarpour, "Network constrained economic dispatch of renewable energy and CHP based microgrids," *International Journal of Electrical Power & Energy Systems,* vol. 110, pp. 144-160, 2019.

[15] Y. Wang, Y. Huang, Y. Wang, M. Zeng, F. Li, Y. Wang*, et al.*, "Energy management of smart micro-grid with response loads and distributed generation considering demand response," *Journal of cleaner production,* vol. 197, pp. 1069-1083, 2018.

[16] M. A. S. Hassan, M. Chen, H. Lin, M. H. Ahmed, M. Z. Khan, and G. R. Chughtai, "Optimization modeling for dynamic price based demand response in microgrids," *Journal of Cleaner Production,* vol. 222, pp. 231-241, 2019.

[17] D. Neves, M. C. Brito, and C. A. Silva, "Impact of solar and wind forecast uncertainties on demand response of isolated microgrids," *Renewable energy,* vol. 87, pp. 1003-1015, 2016.

[18] M. H. Amrollahi and S. M. T. Bathaee, "Techno-economic optimization of hybrid photovoltaic/wind generation together with energy storage system in a stand-alone micro-grid subjected to demand response," *Applied Energy,* vol. 202, pp. 66-77, 2017.

[19] M. H. Imani, P. Niknejad, and M. Barzegaran, "The impact of customers' participation level and various incentive values on implementing emergency demand response program in microgrid operation," *International Journal of Electrical Power & Energy Systems,* vol. 96, pp. 114-125, 2018.

[20] S. Shafiee, H. Zareipour, A. M. Knight, N. Amjady, and B. Mohammadi-Ivatloo, "Risk-constrained bidding and offering strategy for a merchant compressed air energy storage plant," *IEEE Transactions on Power Systems,* vol. 32, pp. 946-957, 2016.

[21] H. Ibrahim, K. Belmokhtar, and M. Ghandour, "Investigation of usage of compressed air energy storage for power generation system improving-application in a microgrid integrating wind energy," *Energy Procedia,* vol. 73, pp. 305-316, 2015.

[22] S. N. Dash, R. K. Padhi, T. Dora, A. Surendar, and K. Cristan, "A robust optimization method for bidding strategy by considering the compressed air energy storage," *Sustainable Cities and Society,* vol. 48, p. 101564, 2019.

[23] J. Zhang, K.-J. Li, M. Wang, W.-J. Lee, H. Gao, C. Zhang*, et al.*, "A bi-level program for the planning of an islanded microgrid including CAES," *IEEE Transactions on Industry Applications,* vol. 52, pp. 2768-2777, 2016.

[24] M. A. Mirzaei, A. Sadeghi-Yazdankhah, B. Mohammadi-Ivatloo, M. Marzband, M. Shafie-khah, and J. P. Catalão, "Integration of emerging resources in IGDT-based robust scheduling of combined power and natural gas systems considering flexible ramping products," *Energy,* vol. 189, p. 116195, 2019.

[25] B. Dey, S. K. Roy, and B. Bhattacharyya, "Solving multi-objective economic emission dispatch of a renewable integrated microgrid using latest bio-inspired algorithms," *Engineering Science and Technology, an International Journal,* vol. 22, pp. 55-66, 2019.

[26] M. Sedighizadeh, M. Esmaili, A. Jamshidi, and M.-H. Ghaderi, "Stochastic multi-objective economic-environmental energy and reserve scheduling of microgrids considering battery energy storage system," *International Journal of Electrical Power & Energy Systems,* vol. 106, pp. 1-16, 2019.

[27] L. He, Z. Lu, L. Pan, H. Zhao, X. Li, and J. Zhang, "Optimal Economic and Emission Dispatch of a Microgrid with a Combined Heat and Power System," *Energies,* vol. 12, p. 604, 2019.

[28] J. Aghaei and M.-I. Alizadeh, "Multi-objective self-scheduling of CHP (combined heat and power)-based microgrids considering demand response programs and ESSs (energy storage systems)," *Energy,* vol. 55, pp. 1044-1054, 2013.

[29] M. Nazari-Heris, S. Abapour, and B. Mohammadi-Ivatloo, "Optimal economic dispatch of FC-CHP based heat and power micro-grids," *Applied Thermal Engineering,* vol. 114, pp. 756-769, 2017.

[30] P. Pourghasem, F. Sohrabi, M. Abapour, and B. Mohammadi-Ivatloo, "Stochastic multi-objective dynamic dispatch of renewable and CHP-based islanded microgrids," *Electric Power Systems Research,* vol. 173, pp. 193-201, 2019.

[31] M. Hemmati, B. Mohammadi-Ivatloo, and A. Soroudi, "Uncertainty management in decision-making in power system operation," in *Decision Making Applications in Modern Power Systems*, ed: Elsevier, 2020, pp. 41-62.

[32] M. Alipour, B. Mohammadi-Ivatloo, and K. Zare, "Stochastic scheduling of renewable and CHP-based microgrids," *IEEE Transactions on Industrial Informatics,* vol. 11, pp. 1049-1058, 2015.

[33] M. Mazidi, N. Rezaei, and A. Ghaderi, "Simultaneous power and heat scheduling of microgrids considering operational uncertainties: A new stochastic p-robust optimization approach," *Energy,* vol. 185, pp. 239-253, 2019.

[34] M. Hemmati, B. Mohammadi-Ivatloo, S. Ghasemzadeh, and E. Reihani, "Risk-based optimal scheduling of reconfigurable smart renewable energy based microgrids," *International Journal of Electrical Power & Energy Systems,* vol. 101, pp. 415-428, 2018.

[35] F. S. Gazijahani and J. Salehi, "Robust design of microgrids with reconfigurable topology under severe uncertainty," *IEEE Trans. Sustainable Energy,* pp. 1-11, 2018.

[36] M. A. Mirzaei, M. Hemmati, K. Zare, M. Abapour, B. Mohammadi-Ivatloo, M. Marzband*, et al.*, "A novel hybrid two-stage framework for flexible bidding strategy of reconfigurable micro-grid in day-ahead and real-time markets," *International Journal of Electrical Power & Energy Systems,* vol. 123, p. 106293, 2020.

[37] S. Esmaeili, A. Anvari-Moghaddam, S. Jadid, and J. M. Guerrero, "Optimal simultaneous day-ahead scheduling and hourly reconfiguration of distribution systems considering responsive loads," *International Journal of Electrical Power & Energy Systems,* vol. 104, pp. 537-548, 2019.

[38] F. Yaprakdal, M. Baysal, and A. Anvari-Moghaddam, "Optimal Operational Scheduling of Reconfigurable Microgrids in Presence of Renewable Energy Sources," *Energies,* vol. 12, p. 1858, 2019.

[39] A. Ajoulabadi, S. N. Ravadanegh, and B. Mohammadi-Ivatloo, "Flexible scheduling of reconfigurable microgrid-based distribution networks considering demand response program," *Energy,* vol. 196, p. 117024, 2020.
[40] R. Kaviani, M. Rashidinejad, and A. Abdollahi, "A milp igdt-based self-scheduling model for participating in electricity markets," in *2016 24th Iranian Conference on Electrical Engineering (ICEE)*, 2016, pp. 152-157.
[41] H. Sadeghian and M. Ardehali, "A novel approach for optimal economic dispatch scheduling of integrated combined heat and power systems for maximum economic profit and minimum environmental emissions based on Benders decomposition," *Energy,* vol. 102, pp. 10-23, 2016.
[42] S. Shafiee, H. Zareipour, and A. Knight, "Considering thermodynamic characteristics of a CAES facility in self-scheduling in energy and reserve markets," *IEEE Transactions on Smart Grid,* 2016.
[43] B. Mohammadi-Ivatloo, H. Zareipour, N. Amjady, and M. Ehsan, "Application of information-gap decision theory to risk-constrained self-scheduling of GenCos," *IEEE Transactions on Power Systems,* vol. 28, pp. 1093-1102, 2012.
[44] M. G. Delgado, J. S. Ramos, S. Á. Domínguez, J. A. T. Ríos, and L. F. Cabeza, "Building thermal storage technology: Compensating renewable energy fluctuations," *Journal of Energy Storage,* vol. 27, p. 101147, 2020.
[45] M. Alipour, K. Zare, H. Seyedi, and M. Jalali, "Real-time price-based demand response model for combined heat and power systems," *Energy,* vol. 168, pp. 1119-1127, 2019.
[46] M. Hemmati, B. Mohammadi-Ivatloo, M. Abapour, and A. Anvari-Moghaddam, "Day-ahead profit-based reconfigurable microgrid scheduling considering uncertain renewable generation and load demand in the presence of energy storage," *Journal of Energy Storage,* vol. 28, p. 101161, 2020.